Hindawi
Mathematical Problems in Engineering
Volume 2017, Article ID 7952152, 9 pages
https://doi.org/10.1155/2017/7952152

Research Article

Efficient Iris Localization via Optimization Model

Qi Wang, Zhipeng Liu, Shu Tong, Yuqi Yang, and Xiangde Zhang

Department of Mathematics, College of Sciences, Northeastern University, Shenyang 110819, China

Correspondence should be addressed to Xiangde Zhang; zhangxiangde@mail.neu.edu.cn

Received 16 July 2017; Accepted 27 November 2017; Published 18 December 2017

Academic Editor: Ivan Giorgio

Iris localization is one of the most important processes in iris recognition. Because of different kinds of noises in iris image, the localization result may be wrong. Besides this, localization process is time-consuming. To solve these problems, this paper develops an efficient iris localization algorithm via optimization model. Firstly, the localization problem is modeled by an optimization model. Then SIFT feature is selected to represent the characteristic information of iris outer boundary and eyelid for localization. And SDM (Supervised Descent Method) algorithm is employed to solve the final points of outer boundary and eyelids. Finally, IRLS (Iterative Reweighted Least-Square) is used to obtain the parameters of outer boundary and upper and lower eyelids. Experimental result indicates that the proposed algorithm is efficient and effective.

1. Introduction

Iris recognition is one of the most reliable biometrics [1–3]. It is widely used in different kinds of applications.

A typical iris recognition system contains several steps, which are iris image acquisition, segmentation, feature extraction, matching, and recognition [4–7]. In these steps, segmentation is the most important and basic process. This step mainly localize four boundaries of iris, which are inner and outer boundaries of iris and upper and lower eyelids.

In fact, it is difficult to obtain accurate and stable iris boundaries under different conditions, such as variable and nonuniform brightness, occlusion of eyelashes and eyelids, specular reflections, and glasses covering. These undetermined factors make iris segmentation difficult. Segmentation has become a major bottleneck in iris recognition system.

The most well-known two iris localization algorithms are integrodifferential (Itg-Diff) operator [4–6] and edge detection combined with Hough transform [7]. They are widely approved by different publications. However, these two methods mainly use gradient information, which are easily affected by different kinds of noises. They are probably not efficient and generate wrong localization under some conditions.

(1) Computation Complexity. The efficiency of Itg-Diff operator is mainly affected by the range of boundary parameters. When the searching space of parameter is large, the localization process has a large computation complexity. The efficiency of Hough transform is mainly affected by the size of parameter space and the count of detected edge pixels. The detected edge generally contains a lot of noises. When too much noise is included or large parameter space is used, the computation process is time-consuming.

(2) Inaccurate Localization of the Outer Boundary of Iris. As the Itg-Diff operator and the edge detection process just depend on gradient information, they are vulnerable to eyelashes, light spot, spectacle frame, and other noises, resulting in wrong localization.

(3) Incorrect Segmentation of the Upper and Lower Eyelids. With the diversity of the equipment, environment, and individuals, the eyelids in captured images differ greatly. This leads to incorrect segmentation of eyelids.

In recent years, many algorithms have been proposed based on the above two classical algorithms. Cui et al. [8] extract the low frequency information of iris image by wavelet transform. They use Itg-Diff operator to segment iris. Sundaram et al. [9] reduce search range of iris and pupil to reduce complexity; then they utilize Hough transform for localization. Other algorithms such as Hooke's Law [10], active contour [11, 12], and histogram analysis [13] also get satisfying

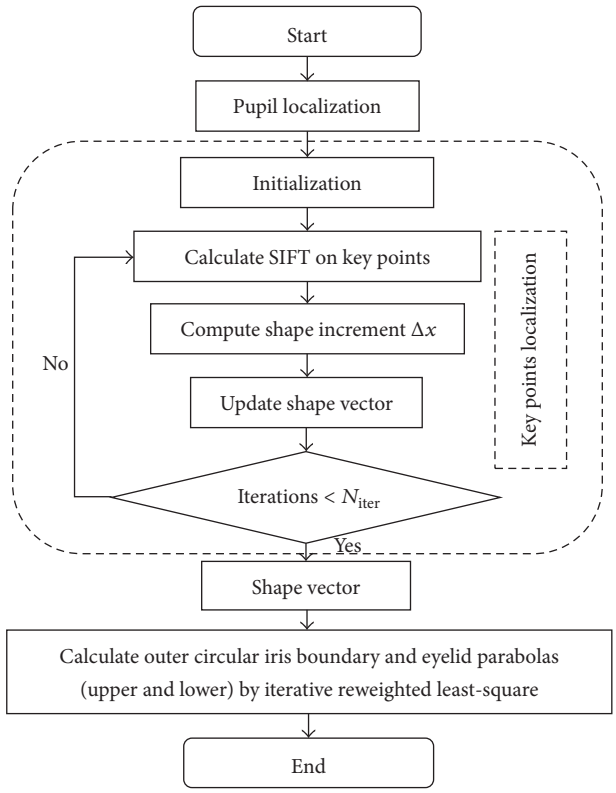

Figure 1: Flow chart of proposed iris localization method.

results. More iris segmentation methods are surveyed by Jan [14].

In fact, these proposed iris segmentation methods mainly depend on gradient information. So the localization process is easily affected by different kinds of noises, generating wrong segmentations. On the other side, the existing noise makes it difficult to estimate the range of boundary parameters. This makes the searching process computation complexity.

Considering that gradient information is easily affected by noises, we try to select more robust features to represent iris boundary.

SIFT (scale-invariant features transform) [15, 16] is a robust and scale-invariant local feature descriptor. Xiong and de la Torre [17] proposed to localize key points of face with SIFT and SDM (Supervised Descend Method) algorithm. Inspired by this paper, we try to use SIFT to extract local feature of iris boundary. The localization process is solved by SDM [17].

Figure 1 shows the flow chart of proposed iris localization method. Firstly, pupil is coarsely located by RST (Radial Symmetry Transform) [18] and the fine boundary is determined by Itg-Diff operator. Then, we extract the SIFT feature of key points on iris's outer boundary and eyelids (upper and lower). Based on these key points, the developed optimization model is solved by SDM. After that, some key points on iris's outer boundary and eyelids (upper and lower) are obtained. The final eyelids and iris boundary are determined by IRLS (Iterative Reweighted Least-Square).

Figure 2 illustrates the whole procedure of the proposed algorithm. Figure 3 shows the comparison between the ideal and obtained localization result by proposed algorithm.

The paper is organized as follows: Section 2 illustrates the mathematical model of localization algorithm. Section 3 present the proposed iris localization method. Section 4 shows the experimental result and analysis. Section 5 concludes the whole paper.

2. Mathematical Model and Related Basis

2.1. Mathematical Model of Iris Localization. Let I be an iris image and $\mathbf{x}$ be a vector of the coordinates of l pixels in the image, $\mathbf{x} = [x_1, y_1, x_2, y_2, \ldots, x_l, y_l]^T$. $\mathbf{x}^*$ is the vector of destination boundaries, which is composed of coordinates of l key points, $\mathbf{x}^* = [x_1^*, y_1^*, x_2^*, y_2^*, \ldots, x_l^*, y_l^*]^T$. Then the localization process is equal to calculating $\triangle x = [x_1^* - x_1, y_1^* - y_1, x_2^* - x_2, y_2^* - y_2, \ldots, x_l^* - x_l, y_l^* - y_l]$, which is illustrated in Figure 4.

Define $\phi(I(\mathbf{x}))$ as the feature vector of $\mathbf{x}$, which is composed of l groups of features on $[x_1, y_1], [x_2, y_2], \ldots, [x_l, y_l]$. Here, ϕ is a feature extraction function, which projects pixels to their corresponding feature descriptor.

With this definition, $\phi(I(\mathbf{x}^*))$ is the feature vector of $\mathbf{x}^*$. Then the localization process is equal to searching for the most similar feature vector $\phi(I(\mathbf{x}))$ to $\phi(I(\mathbf{x}^*))$. Ideally, when the difference between the two feature vectors $\phi(I(\mathbf{x}))$ and $\phi(I(\mathbf{x}^*))$ is small, $\mathbf{x}$ would be close to the target shape vector $\mathbf{x}^*$, which is the expected localization.

Here we use Euclidean distance to measure the similarity of two feature vectors. Then the iris localization procedure is equivalent to minimizing the following objective function:

$$f(\mathbf{x}) = \left\| \phi(I(\mathbf{x})) - \phi(I(\mathbf{x}^*)) \right\|_2^2. \quad (1)$$

Let $\mathbf{x} = \mathbf{x_0} + \mathbf{\Delta x}$, where $\mathbf{x_0}$ is the initial coordinate vector, $\mathbf{\Delta x}$ is the offset from $\mathbf{x}$ to $\mathbf{x_0}$, and (1) can be rewritten as

$$f(\mathbf{x_0} + \mathbf{\Delta x}) = \left\| \phi(I(\mathbf{x_0} + \mathbf{\Delta x})) - \phi(I(\mathbf{x}^*)) \right\|_2^2. \quad (2)$$

When the feature extracting function ϕ is nonlinear, the minimization of (2) is a nonlinear programming problem. The final shape vector $\mathbf{x_0} + \mathbf{\Delta x}$ can be obtained by solving the following optimization problem:

$$\widehat{\mathbf{\Delta x}} = \arg\min \quad \left\| \phi(I(\mathbf{x_0} + \mathbf{\Delta x})) - \phi(I(\mathbf{x}^*)) \right\|_2^2. \quad (3)$$

Then the final localization shape vector is

$$\widehat{\mathbf{x}} = \mathbf{x_0} + \widehat{\mathbf{\Delta x}}. \quad (4)$$

2.2. SIFT Feature of Boundary. SIFT is a commonly used image local feature descriptor [15, 16]. It is widely used in many different computer vision problems [19]. In this paper, we adopt a similar strategy as [17], extract SIFT feature vectors of the key points on iris boundary for localization. Figure 5 illustrates the SIFT feature of different points on iris boundary. This figure indicates that the given four points (labeled as 1–4) on iris outer boundary have similar SIFT features.

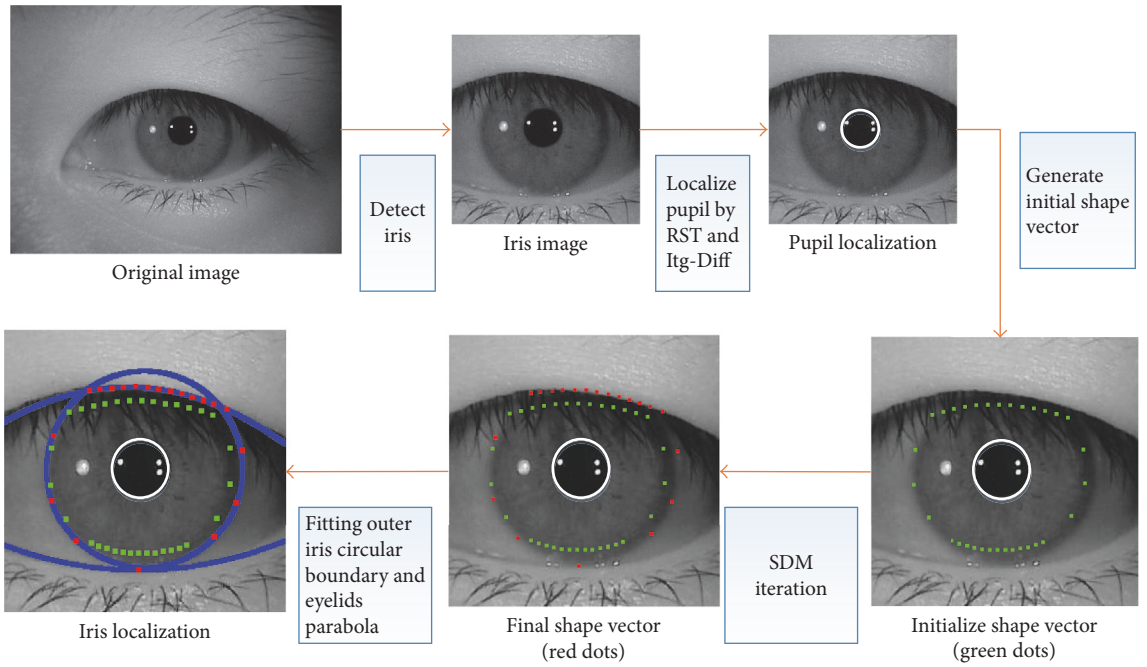

FIGURE 2: An illustration of iris localization process. The blue curves are the fitting circles and parabolas. The green points are the initialized shape of the localization. The red points are the final shape of the procedure.

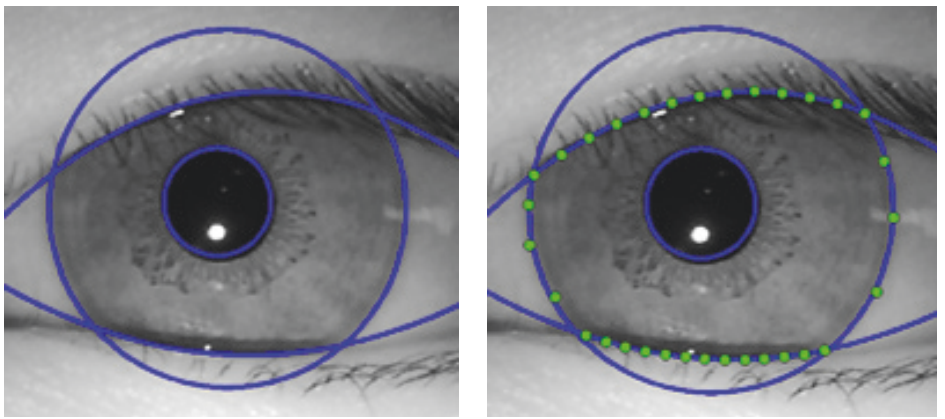

(a) (b)

FIGURE 3: Iris segmentation. (a) Ideal iris localization and (b) localization result by proposed method.

2.3. SDM Algorithm. By substituting the SIFT feature vector into the optimization problem in (3), a nonlinear programming problem is obtained. The SDM Algorithm [17] adopts supervised learning to obtain the optimal iteration vector from the current shape vector to the target. It is an iterative algorithm for solving the optimization problem.

This algorithm establishes a linear regression model between the offset of the shape vector $\mathbf{\Delta x} = \mathbf{x}^* - \mathbf{x}$ and the feature $\phi(I(\mathbf{x}))$ of the current shape vector $\mathbf{x}$

$$\mathbf{\Delta x} = R\phi\left(I\left(\mathbf{x}\right)\right) + b. \tag{5}$$

Then the current shape vector $\mathbf{x}$ and the offset vector $\mathbf{\Delta x}$ can be calculated iteratively, to obtain the desired position vector: $\mathbf{x} := \mathbf{x} + \mathbf{\Delta x}$.

In order to reduce the possibility of falling in a local minimum, SDM adopts several iterations to obtain a series of R_k and b_k

$$\arg\min_{R_k, b_k} \sum_I \sum_i \left\| \Delta \mathbf{x}_*^{ki} - R_k \phi\left(I\left(\mathbf{x}_k^i\right)\right) - b_k \right\|^2, \tag{6}$$

where k is the number of iterations and $\mathbf{x}_k^i$ is the coordinate of the ith point of shape vector at the kth iteration.

3. Proposed Method

3.1. Pupil Determination. When iris images are taken by the near-infrared equipment, there is a large difference between

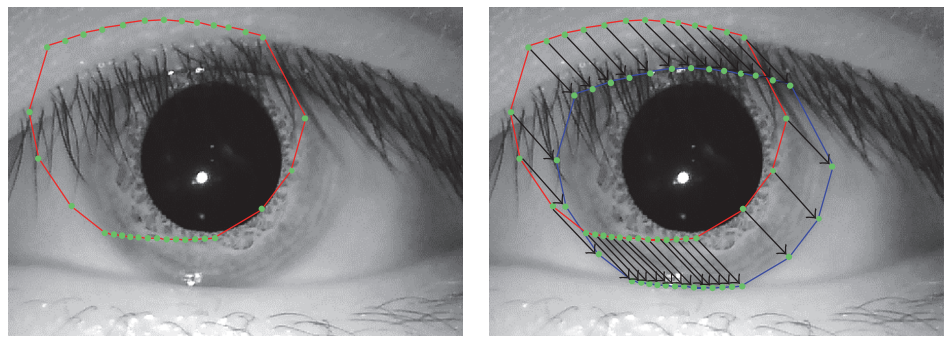

(a) Initial shape of iris outer boundary (b) Initial and final shape of outer boundary

FIGURE 4: Illustration of iris localization process: (a) initial shape of iris boundary; (b) the relative position of initial and localized iris boundary.

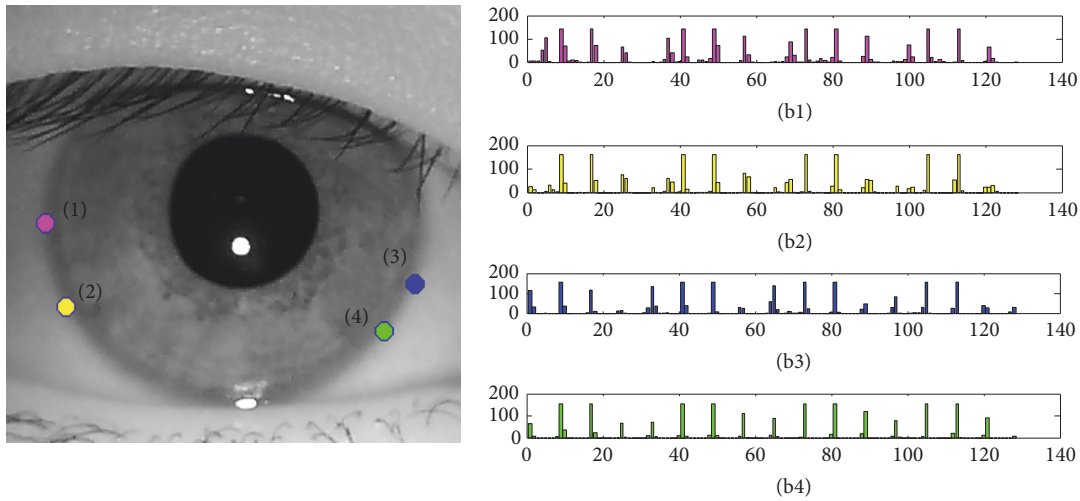

(a) (b)

FIGURE 5: SIFT feature of different points. (a) positions of selected edge points; (b) SIFT feature of selected four points.

pupil and iris. Here, we adopt a "coarse-to-fine" pupil localization strategy. Firstly, a rough pupil position is obtained by RST [20]; then the accurate localization is obtained by Itg-Diff operator.

Itg-Diff operator [4–6] is proposed by Daugman. The formula is given as follows:

$$\max_{(a,b,r)} \left| G_\sigma(r) * \frac{\partial}{\partial r} \oint_{a,b,r} \frac{I(x,y)}{2\pi r} ds \right|, \tag{7}$$

where $G_\sigma(r)$ is a smooth function, $*$ is convolution operator, $I(x,y)$ is the image, (a,b) is the center of the circular boundary, and r is the radius.

The operator calculates annular gray difference along the radial direction in iris image and searches the max difference.

3.2. SDM Learning. In this paper, we select 32 key points on the outer boundary of iris. Figure 6 illustrates the positions of these points. Among them, upper and lower eyelids contain 13 points separately, and the left and right arcs of the iris boundary have 4 points, respectively. Figure 6(a) is the training image with marked points on both upper and lower eyelids, where the points 1st, 13th, 14th, and 26th are the intersection points of the eyelids and outer edge of iris, respectively; Figure 6(b) is the training image without intersection of the lower eyelids and iris, where the lowest point on the outer edge of the iris is marked as the points 14th to 26th; Figure 6(c) is the training image without intersection of the upper eyelids and iris, where the highest point on the outer edge of the iris is marked as the points 1th to 13th; Figure 6(d) shows the average shape vector of all training samples. SIFT features of the marked points are calculated for every image in the database and R_k and b_k, which are saved as the learned parameters of linear regression, are obtained by solving (6).

3.3. Key Points Localization. In localization process, the outer boundary of iris is initialized based on the parameters of

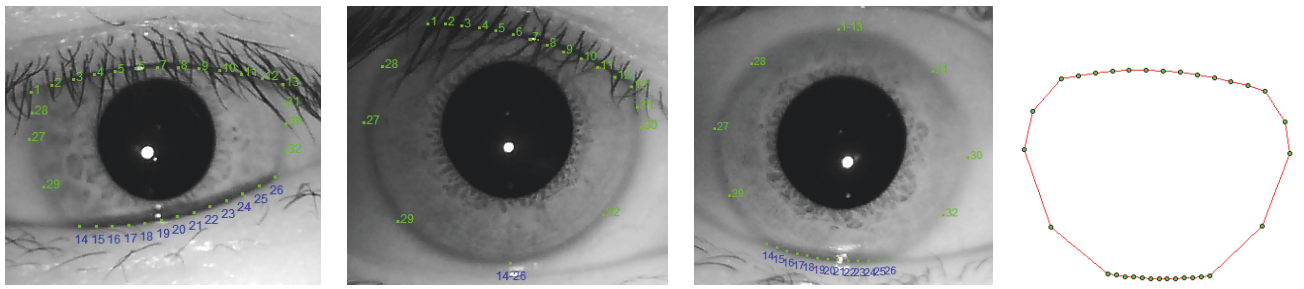

(a) (b) (c) (d)

Figure 6: Examples of labeled key points. (a) Labeled key points on iris occluded by upper and lower eyelids. (b) Labeled key points on iris occluded by upper eyelid. (c) Labeled key points on iris occluded by lower eyelid. (d) Mean shape of all labeled key points.

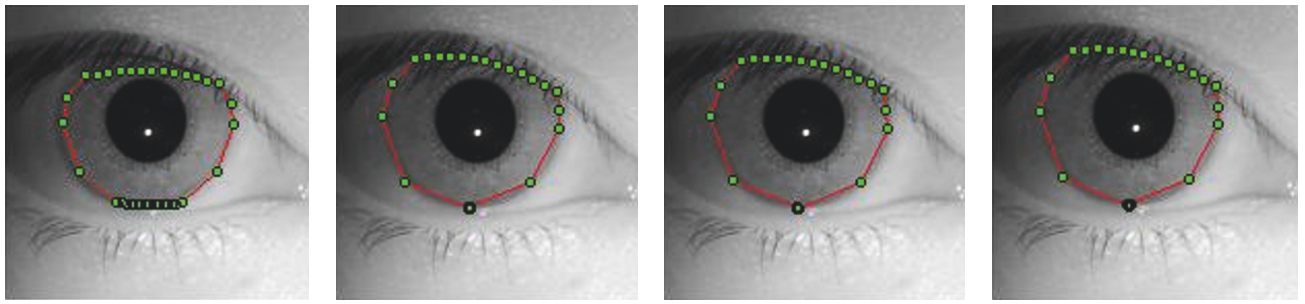

(a) (b) (c) (d)

Figure 7: Illustration of iteration steps. (a) Initialization of key points. (b) Key points after one iteration. (c) Key points after twice iterations. (d) Key points after triple iterations.

pupil localization and the average shape. Figure 7 illustrates the changing process of shape after different iteration steps. Figure 7(a) demonstrates the initial key points. Figures 7(b), 7(c), and 7(d), respectively, show the localized shapes, which are obtained after once, twice, and triple iterations.

The iris image we used is scaled down to 1/4 side length. The iteration number $N_{\text{iter}} = 3$.

3.4. Estimating Boundaries. With these key points obtained by SDM, IRLS algorithm is adopted to locate the iris and eyelids boundary. The outer boundary of iris and eyelids (up and down) are fitted by circle and parabolas separately.

3.4.1. Linearization of Circle Equation. A standard equation of circle is

$$x^2 + y^2 - ax - by - c = 0, \tag{8}$$

where x and y are the horizontal and vertical coordinates of the point on the circle and a, b, and c are the parameters. The circular equation can be written as

$$x^2 + y^2 = \begin{pmatrix} 1 & x & y \end{pmatrix} \begin{pmatrix} c \\ a \\ b \end{pmatrix}. \tag{9}$$

Let $Y = x^2 + y^2$, $X = \begin{pmatrix} 1 & x & y \end{pmatrix}$, $\beta = \begin{pmatrix} c & a & b \end{pmatrix}^T$; then the equation of circle can be written as

$$Y = X\beta. \tag{10}$$

3.4.2. Linearization of Parabolic Function. A standard parabolic function can be given as follows:

$$y = dx^2 + ex + p. \tag{11}$$

Then the function turns to be

$$y = \begin{pmatrix} 1 & x & x^2 \end{pmatrix} \begin{pmatrix} p \\ e \\ d \end{pmatrix}. \tag{12}$$

Let $Y' = y$, $X' = \begin{pmatrix} 1 & x & x^2 \end{pmatrix}$, $\beta' = \begin{pmatrix} p & e & d \end{pmatrix}^T$; then the parabolic function could be given as

$$Y' = X'\beta'. \tag{13}$$

3.4.3. Estimating Parameter by IRLS. When the circular and parabolic functions are illustrated as (10) and (13), the original nonlinear functions are turned to be linear. The parameters of these functions can be solved by least-square related methods. Here we use IRLS [21] to estimate these unknown parameters.

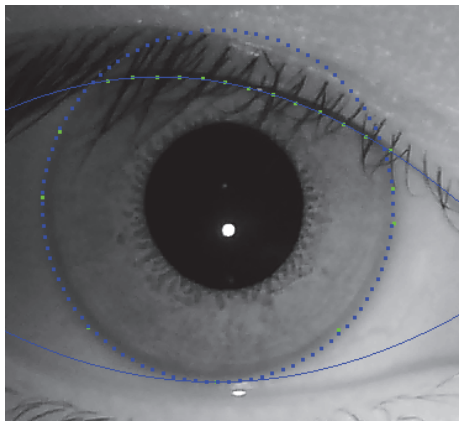

Figure 8: Segmentation result.

Assume the deviation of the ith point is ϵ_i, $\epsilon_i = Y_i - X_i\beta$. To make the regression robust, we use bisquare function as the weight function, which is $\omega_i(\beta) = (\epsilon_i < b)(1 - (\epsilon_i/b)^2)^2$; b is bandwidth. Then the following optimization problem would be obtained by minimizing the weighted square error

$$\arg\min_{\beta} \quad \sum_i \omega_i(\beta)\left(Y_i - X_i\beta\right)^2, \tag{14}$$

where (X_i, Y_i) is the coordinates of the ith key points obtained by SDM.

Here we use IRLS to solve (14). The iterative function is

$$\beta^{(t+1)} = \arg\min_{\beta} \sum_i \omega_i\left(\beta^{(t)}\right)\left(Y_i - X_i\beta^{(t)}\right)^2. \tag{15}$$

The solving process is realized by a Matlab built-in function. Figure 8 illustrates the key points and final localized boundaries. The key points on outer iris boundary and the upper and lower eyelids are obtained by SDM. The continuous boundaries are calculated by IRLS.

4. Experimental Result and Analysis

The proposed algorithm was tested on a monocular iris acquisition device TCI 311, which is manufactured by Techshino Technology Inc., Beijing. It is a near infrared camera with prime lens. The capturing distance is 8–10 cm. The resolution of the iris image is 640 ∗ 480. We construct an iris database containing 700 images by this device.

The experiment is carried out on a computer with Intel Core i5 CPU, 2 GB RAM, and the Operating System is Windows 7 Professional 32-bit. The algorithm is coded in Matlab 2014b and C++.

In our experiment, the training and verification images are randomly selected from the image database for cross-validation. The ratio of training and verified images is 7 : 3.

Table 1: Segmentation accuracy of different methods.

Localized part	Itg-Diff	Proposed algorithm
Iris	99.2%	99.5%
Eyelids	99.6%	99.6%

The error rate $\rho_{\text{cer}}^{i,j}$ and the failure rate ρ_{cfr}^{j} of the localization accuracy are defined as follows:

$$\rho_{\text{cer}}^{i,j} = \frac{\left|x_{t_i}^j - x_{T_i}^j\right|}{\max\left(D_h^j, D_w^j\right)},$$
$$\rho_{\text{cfr}}^{j} = \frac{\max_i \left|x_{t_i}^j - x_{T_i}^j\right|}{\max\left(D_h^j, D_w^j\right)} = \max_i \rho_{\text{cer}}^{i,j}, \tag{16}$$

where $x_{t_i}^j$ and $x_{T_i}^j$ denote the test position and the true position of the ith point on the jth sample image, respectively. $|\cdot|$ represents the Euclidean distance. D_h^j and D_w^j denote the length and width of the minimum circumscribed rectangle of all the key points on the jth sample image. According to the definition, $\rho_{\text{cer}}^{i,j}$ measures the sample point error and ρ_{cfr}^{j} is the location failure rate.

The cumulative error rate is defined as follows:

$$\rho_{\text{cer}} = \sum_{i,j} I\left(\rho_{\text{cer}}^{i,j} < \alpha\right). \tag{17}$$

The cumulative failure rate is defined as follows:

$$\rho_{\text{cfr}} = \sum_{j} I\left(\rho_{\text{cfr}}^{j} < \beta\right). \tag{18}$$

Here, α and β are the evaluation criteria, and I is an indicator function:

$$I\,(\text{REGEXP}) = \begin{cases} 1, & \text{if REGEXP is TRUE,} \\ 0, & \text{otherwise.} \end{cases} \tag{19}$$

Figure 9 shows ρ_{cer} and ρ_{cfr} curves. Figure 10 shows the localization result by proposed method. Table 1 illustrates the performance comparison of iris boundary and eyelids localization by Itg-Diff and proposed algorithm. Figure 11 compares the results obtained by Itg-Diff operator and the proposed method, where the first line is the result of the Itg-Diff operator and the second line is the result of the proposed method. These comparisons demonstrate that the proposed method has more stable localization performance than Itg-Diff operator in noisy iris image, especially with large light spots, spectacle frames, and so on.

That is because the Itg-Diff operator relies on the gradient information on 3 × 3 neighborhood. It is sensitive to local intensity variation. When iris images contain light spot, eyelid, eyelash, eyeglass frame, and so on, the Itg-Diff operator likely produces wrong segmentations.

While SIFT feature is generated on a relative large local area, it is more robust to image rotation, brightness variation,

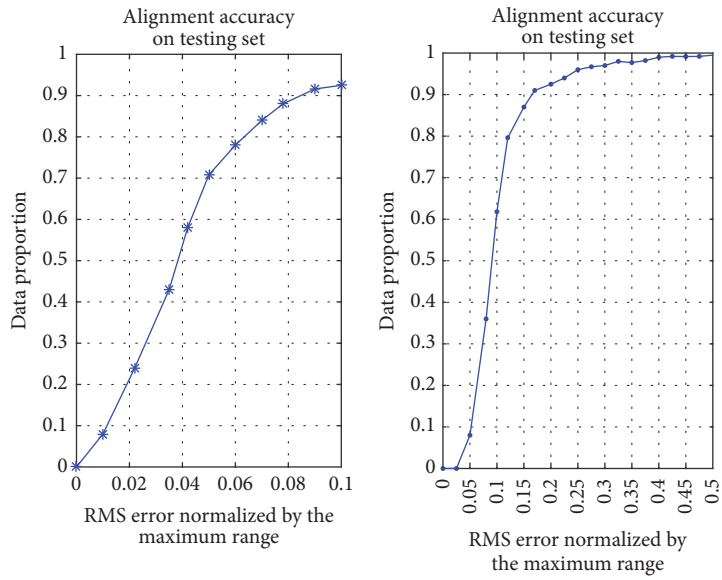

Figure 9: Cumulative error curves on testing set. (a) Error proportion via cumulative Root Mean Square. (b) Error proportion via cumulative failure rate.

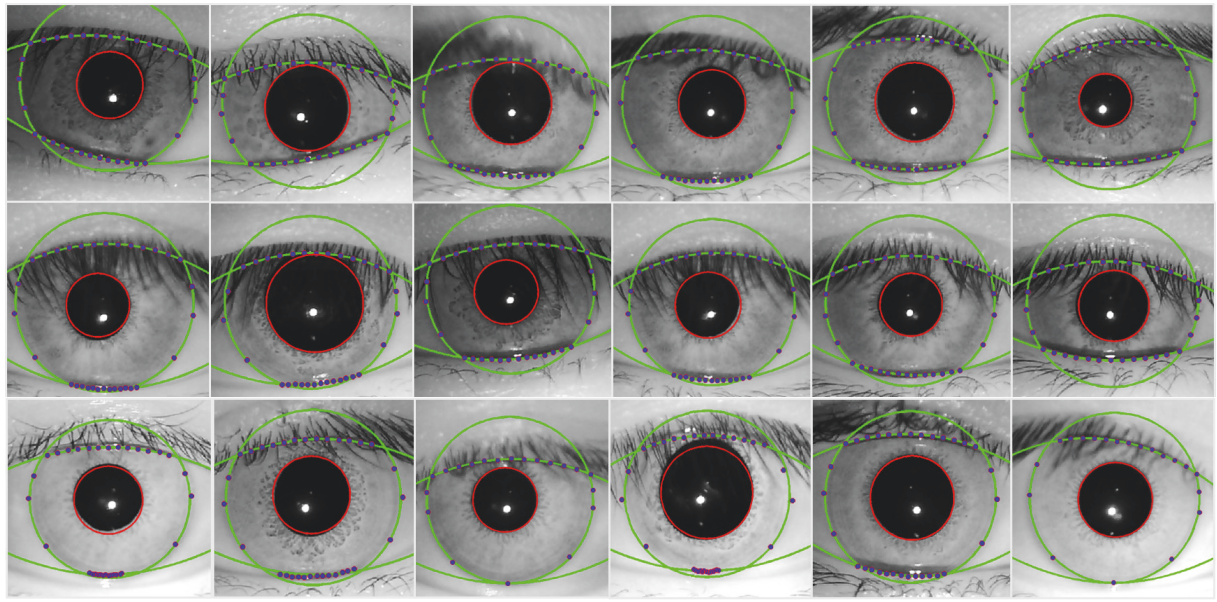

Figure 10: Segmentation results by proposed method.

scale scaling, and noise than gradient information. This enhances the robustness of localization algorithm.

Table 2 shows the run-time of the proposed method and the other two methods. It takes an average of 26.7 ms to localize an iris image in our experiment, which is much efficient than compared algorithms.

Table 2: Computation time of different methods.

Methods	Itg-Diff	ED + Radon [22]	Proposed algorithm
Time	600 ms	153.7 ms	26.7 ms

5. Conclusions

In this paper, an efficient iris location algorithm based on optimization model is proposed. Firstly, RST and Itg-Diff operator are used to locate pupil; then the key points on the outer boundary of iris are represented by SIFT features and located by SDM. Finally, the parameters of the outer boundary of the iris are determined by IRLS.

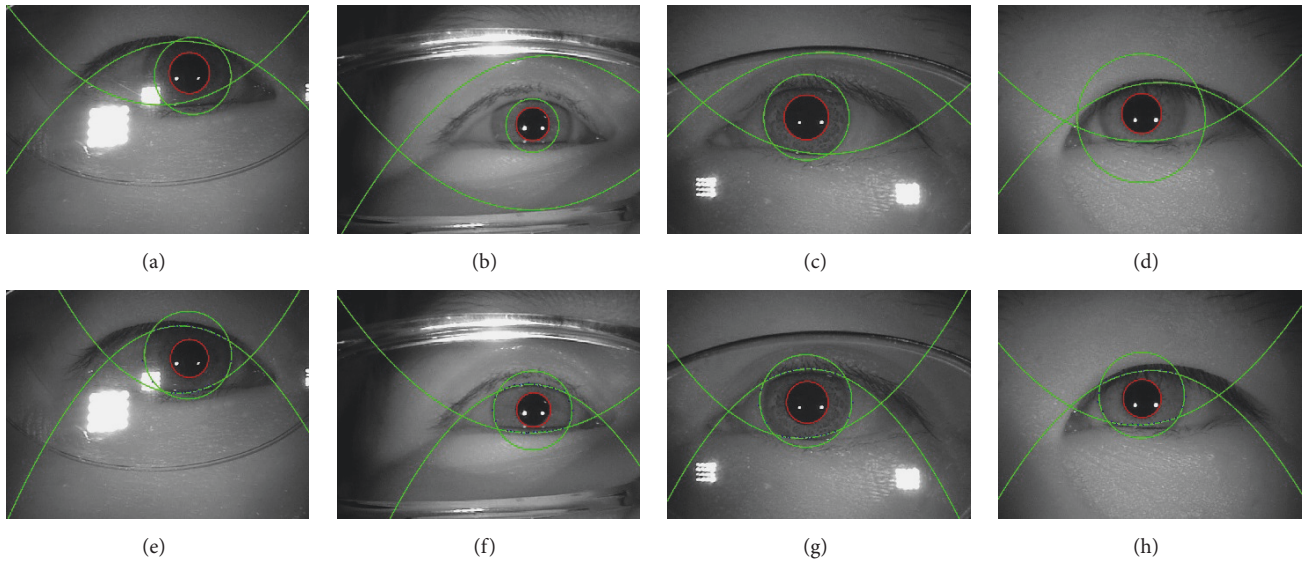

Figure 11: Segmentation results by different methods (the first and second rows are obtained by Itg-Diff and proposed method separately).

The main contribution of this paper could be summarized as follows. (1) An optimization model is developed for iris localization. (2) SIFT feature is used for iris boundary representation, which is more robust than gradient information. (3) SDM algorithm is introduced to solve the iris localization problem, which can generate the key points of outer boundary of iris.

Experimental results indicate that the proposed method can localize the outer boundary of iris and the upper and lower eyelids efficiently and robustly.

Conflicts of Interest

The authors declare that they have no conflicts of interest.

Acknowledgments

This work is supported by National Natural Science Funds of China, no. 61703088, the Doctoral Scientific Research Foundation of Liaoning Province, no. 20170520326, and "the Fundamental Research Funds for the Central Universities," N160503003.

References

[1] J. Daugman, "Statistical richness of visual phase information: update on recognizing persons by iris patterns," *International Journal of Computer Vision*, vol. 45, no. 1, pp. 25–38, 2001.

[2] J. Daugman, "Demodulation by complex-valued wavelets for stochastic pattern recognition: how iris recognition works," in *Wavelet analysis and its applications (WAA). Vol. 1, 2*, pp. 511–530, World Sci. Publ., River Edge, NJ, USA, 2003.

[3] R. P. Wildes, "Iris recognition: an emerging biometrie technology," *Proceedings of the IEEE*, vol. 85, no. 9, pp. 1348–1363, 1997.

[4] J. G. Daugman, "High confidence visual recognition of persons by a test of statistical independence," *IEEE Transactions on Pattern Analysis and Machine Intelligence*, vol. 15, no. 11, pp. 1148–1161, 1993.

[5] J. Daugman, "How iris recognition works," *IEEE Transactions on Circuits and Systems for Video Technology*, vol. 14, no. 1, pp. 21–30, 2004.

[6] Z. Xiangde, D. Xiaopeng, W. Qi, and Y. Sun, "Location algorithm of rgb iris image based on integro-differential operators," *Journal of Northeastern University: Natural Science*, vol. 32, no. 11, pp. 1550–1553, 2011.

[7] R. P. Wildes, J. C. Asmuth, G. L. Green et al., "A machine-vision system for iris recognition," *Machine Vision and Applications*, vol. 9, no. 1, pp. 1–8, 1996.

[8] J. Cui, Y. Wang, T. Tan, L. Ma, and Z. Sun, "A fast and robust iris localization method based on texture segmentation," in *Proceedings of the Biometric Technology for Human Identification*, pp. 401–408, USA, April 2004.

[9] R. M. Sundaram, B. C. Dhara, and B. Chanda, "A fast method for iris localization," in *Proceedings of the 2nd International Conference on Emerging Applications of Information Technology, EAIT 2011*, pp. 89–92, India, February 2011.

[10] Z. He, T. Tan, and Z. Sun, "Iris localization via pulling and pushing," in *Proceedings of the 18th International Conference on Pattern Recognition, ICPR 2006*, pp. 366–369, China, August 2006.

[11] J. Daugman, "New methods in iris recognition," *IEEE Transactions on Systems, Man, and Cybernetics, Part B: Cybernetics*, vol. 37, no. 5, pp. 1167–1175, 2007.

[12] J. Koh, V. Govindaraju, and V. Chaudhary, "A robust iris localization method using an active contour model and hough transform," in *Proceedings of the 2010 20th International Conference on Pattern Recognition, ICPR 2010*, pp. 2852–2856, Turkey, August 2010.

[13] K. Grabowski, W. Sankowski, M. Zubert, and M. Napieralska, "Reliable Iris Localization Method With Application To Iris Recognition In Near Infrared Light," in *Proceedings of the International Conference Mixed Design of Integrated Circuits and System, 2006. MIXDES 2006.*, pp. 684–687, Gdynia, Poland.

[14] F. Jan, "Segmentation and localization schemes for non-ideal iris biometric systems," *Signal Processing*, vol. 133, pp. 192–212, 2017.

[15] D. G. Lowe, "Object recognition from local scale-invariant features," in *Proceedings of the 7th IEEE International Conference on Computer Vision (ICCV '99)*, vol. 2, pp. 1150–1157, Kerkyra, Greece, September 1999.

[16] D. G. Lowe, "Distinctive image features from scale-invariant keypoints," *International Journal of Computer Vision*, vol. 60, no. 2, pp. 91–110, 2004.

[17] X. Xiong and F. de la Torre, "Supervised descent method and its applications to face alignment," in *Proceedings of the 26th IEEE Conference on Computer Vision and Pattern Recognition (CVPR '13)*, pp. 532–539, June 2013.

[18] W. Zhang, B. Li, X. Ye, and Z. Zhuang, "A Robust Algorithm for Iris Localization Based on Radial Symmetry," in *Proceedings of the 2007 International Conference on Computational Intelligence and Security Workshops (CISW 2007)*, pp. 324–327, Harbin, Heilongjiang, China, December 2007.

[19] H. Zhou, Y. Yuan, and C. Shi, "Object tracking using SIFT features and mean shift," *Computer Vision and Image Understanding*, vol. 113, no. 3, pp. 345–352, 2009.

[20] W. Zhang, X. Ye, B. Li, P. Yao, and Z. Zhuang, "A robust iris localization algorithm for non-ideal capturing conditions," *Pattern Recognition and Artificial Intelligence*, vol. 20, no. 5, pp. 675–680, 2007.

[21] C. S. Burrus, *Iterative reweighted least squares*, https://cnx.org/contents/krkDdys0 @12/Iterative-Reweighted-Least-Squ.

[22] C.-L. SHI and L.-X. JIN, "Investigation of the algorithm for iris localization," *Computer Science*, vol. 9, p. 067, 2010.